# A Total Variation Wavelet Inpainting Model with Multilevel Fitting Parameters *

Tony F. Chan † Jianhong Shen ‡ Hao-Min Zhou §

**Abstract**

In [14], we have proposed two total variation (TV) minimization wavelet models for the problem of filling in missing or damaged wavelet coefficients due to lossy image transmission or communication. The proposed models can have effective and automatic control over geometric features of the inpainted images including sharp edges, even in the presence of substantial loss of wavelet coefficients, including in the low frequencies. In this paper, we investigate a modification of the model for noisy images to further improve the recovery properties by using multi-level parameters in the fitting term. Some new numerical examples are also shown to illustrate the effectiveness of the recovery.

## 1 Introduction

In [14], we have studied an image inpainting problem ( filling in missing or damaged regions in images) for which data loss occurs in the wavelets domain. The primary motivation for us to study wavelet based image inpainting is that more images are formatted and stored in terms of wavelet coefficients, due to the current international compression standard JPEG2000, which is largely based on wavelet transforms. Minor damages to compact discs coding JPEG2000 image files and data loss during wireless transmission processes, for example, could both result in the need for filling-in the missing information in the wavelet domain instead of the pixel domain.

The notion of *digital image inpainting* was invented in [4], where the authors pioneered a novel inpainting technique based on a 3rd order nonlinear PDE. This work has stimulated the recent wave of interest in geometric image interpolation and inpainting problems, for example, variational PDE models [11, 12, 13, 23], Navier-Stokes equation and fluid dynamic system related methods [3], landmark based inpainting [26], texture inpainting [5], inpainting by vector fields and gray levels [2], inpainting by corresponding maps [18], and morphological component analysis for cartoon and texture inpainting [22]. The image inpainting is essentially an interpolation problem, and thus directly overlaps with many other important tasks in computer vision and image processing, including image replacement [24], disocclusion[30, 32], zooming and superresolution [12, 28], and error concealment [25, 36].

As demonstrated in [14], working in the wavelet domain, instead of the pixel domain, changes the nature of the inpainting problem, since damages to wavelet coefficients can create correlated damage patterns in the pixel domain. For instance, for wavelet based image inpainting problems, there usually exists no corresponding regular geometric inpainting pixel regions, which are however necessary for many PDE-based inpainting models in pixel domains. Besides, depending on the scales or resolutions, missing or damaged wavelet coefficients could cause degradation wide spread in the pixel domain. That is, even a few coefficients can potentially affect all pixels. Moreover, unlike denoising problems in which the perturbation in the pixel domain is mostly homogeneous, the pixel value degradation in wavelet inpainting problems is usually inhomogeneous (different regions can suffer

*Research supported in part by grants ONR-N00014-03-1-0888, NSF DMS-9973341, DMS-0202565 and DMS-0410062, and NIH contract P 20 MH65166.

†Department of Mathematics, the University of California, Los Angeles, CA90095-1555. email:chan@math.ucla.edu.

‡Department of Mathematics, the University of Minnesota, 206 Church St. SE Minneapolis, MN 55455. email:jhshen@math.umn.edu.

§School of Mathematics, Georgia Institute of Technology, Atlanta, GA 30332. email:hmzhou@math.gatech.edu.

different level of damages). This new phenomenon demands different treatments in different regions in the pixel domain.

To meet the challenges of the wavelet inpainting problems, we have proposed two variational wavelet models that combine the total variation (TV) minimization techniques with wavelet representations in [14]. One primary motivation to use variational PDE techniques for the wavelet inpainting problems is their remarkable success in numerous applications including segmentation [31, 9, 15, 37], restoration [16, 33], compression [10, 17, 20], zooming [29], and conventional image inpainting [3, 4, 11, 13, 23]. In addition, recent efforts by different groups which aim to combine PDE techniques with wavelets have demonstrated the great potential of gaining advantages from both fields of wavelets and PDE techniques [17, 21, 6, 34, 27, 7, 8].

In [14], we have carefully investigated the existence and uniqueness of the proposed models. The associated Euler-Lagrange equations lead to nonlinear partial differential equations (PDE's) in the wavelet domain, and proper numerical algorithms and schemes are designed to handle their computation. We have also demonstrated that the models can have effective and automatic control over geometric features of the inpainted images including sharp edges, even in the presence of substantial loss of wavelet coefficients, including in the low frequencies.

In this paper, we further extend the proposed model for noisy images to allow multilevel parameter selections for the fitting term in the objective functional. This modification is based on the observation that noise affects different wavelet frequencies differently due to the multiresolution structures of wavelet decompositions, For instance, it is easy to see that noise is more visible in the fine resolutions and less noticeable in the coarser scales because it can be averaged out by the low pass filters. Thus, it is natural to use different fitting parameters on different resolutions to eliminate the noise more effectively. Besides, we show some new examples to illustrate that the model can retain geometrical features regardless the inpainting regions are random or deterministic in the wavelet domain.

This paper is arranged as follows. In Section 2, we discuss the modification of the model for the wavelet based inpainting problems, and derive its Euler-Lagrange equation. We present a time marching numerical scheme for solving the Euler-Lagrange equation, and show numerical examples in Section 3 to demonstrate the remarkable inpainting ability of the model.

## 2 A TV Wavelet Inpainting Model with Multilevel Fitting Parameters

In this section, we present a modification of the TV regularized wavelet based image inpainting model for noisy images proposed in [14] by using multilevel parameters in the fitting term.

We start with a standard image model,

$$z(x) = u_0(x) + n(x), \tag{1}$$

where $u_0(x)$ is the original noise free image and $n(x)$ the Gaussian white noise. We assume that the size of the image is $n \times m$. Let us denote the standard orthogonal wavelet transform of $z(x)$ by,

$$z(\alpha, x) = \sum_{j,k} \alpha_{j,k} \psi_{j,k}(x), \qquad j \in \mathbf{Z},\ k \in \mathbf{Z}^2. \tag{2}$$

In wavelet based image representations, the coefficients $\alpha = \{\alpha_{j,k}\}$ are the values being stored. Here we notice that the low and high frequency (or scale) coefficients are not distinguished, while standard wavelet representations usually need to separate them. One reason to do so is for simplicity. A different reason is that we allow the missing or damaged coefficients to be in both low and high frequency ranges. The proposed model can automatically handle them differently if they belong to different frequency ranges, even though low frequency coefficients have completely different properties than the high frequency ones.

Damages (scratches and scars) in the wavelet domain cause loss of wavelet coefficients of $z(x)$ on an index set $I$, i.e., $\{\alpha_{j,k}\}$'s with $(j,k) \in I$ represent those wavelet components missing or damaged. The task of wavelet inpainting is to restore the missing coefficients in a proper manner, so that the image will have as much information being restored as possible.

We have proposed the following TV minimization wavelet inpainting model to restore the wavelet coefficients in $I$ while removing the noise in wavelet coefficients located outside $I$.

**TV Wavelet Inpainting Model** (for noisy images):

$$\min_{\beta_{j,k}} F(u,z) = \int_{\mathbf{R}^2} |\nabla_x u(\beta, x)| dx + \sum_{(j,k)} \lambda_{j,k} (\beta_{j,k} - \alpha_{j,k})^2, \tag{3}$$

and the parameter $\lambda_{(j,k)}$ in the fitting term is zero if $(j,k) \in I$, the missing index set; otherwise, it equals a positive constant $\lambda$ selected depending on the noise level in the known coefficients.

We use the total variation (TV) norm in (3) because it can retain sharp edges while reducing the noise and other oscillations, such as Gibbs' phenomena, in the reconstruction [17].

We want to point out that the parameter $\lambda$ is taken to be zero in the inpainting regions in the wavelet domain, in contrast to the standard denoising and compression models, where $\lambda$ is usually taken to be a constant. This difference essentially puts no constraint on the missing wavelet coefficients so that they can change freely, and therefore restore the missing information.

It is known that $\lambda$ actually controls the smallest scale of features which are preserved in image processing [35]. That is, for a given value of $\lambda$, there exists a size (depending on the intensity level and area) of features such that the model treats all features smaller than this size as oscillations and eliminates them, while preserving features which are larger than this critical scale.

On the other hand, it is easy to observe that noise affects wavelet coefficients in different frequency subbands differently. For instance, Low pass wavelet filters usually have smoothing properties and can average out high frequency noise. Thus, the coefficients in low frequency subbands are less noisy comparing to the ones in high frequencies. Therefore, it is natural to use different parameter values $\lambda$ to remove the noise in different subbands. In this paper, we propose to use

$$\lambda_{j,k} = C_j, \tag{4}$$

where $C_j$ may be a different constant for each subband $j$.

With the new selections of multilevel parameter $\lambda_{j,k}$, the minimizers of (3) are certainly different from the ones obtained by using constant $\lambda$ for every frequency range. However, this modification still retains the basic properties of the original TV wavelet inpainting model. For example, the existence and non-uniqueness of the minimizers can be obtained by adapting the analysis in [14] properly. More importantly, this modification preserves the geometrical properties of variational PDE techniques, and is able to restore the damaged edge and shape information effectively.

Following the derivations in [14], we also get that the minimizers of (3) with multilevel fitting parameters must satisfy the Euler-Lagrange equation which is stated as,

$$-\int_{\mathbf{R}^2} \nabla \left( \frac{\nabla u}{|\nabla u|} \right) \psi_{j,k}(x) dx + 2\lambda_{j,k}(\beta_{j,k} - \alpha_{j,k}) = 0. \tag{5}$$

This equation can be used as the starting point for us to design numerical schemes to achieve the minimizers, which we shall address in the next section.

# 3 Numerical Algorithm and Examples

One way to find the minimizers of (3) is to design a time marching scheme for the Euler-Lagrange equation (5). This is based on the gradient descent approach similar to the one used in [33]. For this purpose, we introduce an artificial time variable and solve the following evolution equation to the steady state,

$$(\beta_{j,k})_t = \int \nabla \left( \frac{\nabla u}{|\nabla u|} \right) \psi_{j,k}(x) dx - 2\lambda_{j,k}(\beta_{j,k} - \alpha_{j,k}). \tag{6}$$

At the steady states where $(\beta_{j,k})_t = 0$, the gradient flow (6) is reduced to the Euler-Lagrange equation (5).

The following described algorithm is based on a simple explicit finite difference scheme.

We first note that the most important term to calculate in the equation (5) is the nonlinear term that projects the curvature onto wavelet basis functions

$$\text{WCURV} \equiv \int \nabla \left( \frac{\nabla u}{|\nabla u|} \right) \psi_{j,k}(x) dx.$$

This is computed using the following straightforward procedure similar to the pseudo-spectral methods,
**Procedure I:** (Compute the curvature projections onto the wavelet basis)

(i) Use the inverse wavelet transform IWT to reconstruct $u$ as

$$u = \text{IWT}(\beta), \tag{7}$$

(ii) For all $(i, j)$, compute

$$\begin{aligned} \text{curv}_{i,j} &= D_1^- \left( \frac{D_1^+ u_{i,j}}{\sqrt{|D_1^+ u_{i,j}|^2 + |D_2^+ u_{i,j}|^2 + \epsilon}} \right) \\ &\quad + D_2^- \left( \frac{D_2^+ u_{i,j}}{\sqrt{|D_1^+ u_{i,j}|^2 + |D_2^+ u_{i,j}|^2 + \epsilon}} \right), \end{aligned} \tag{8}$$

where $D_k^+$, $D_k^-$ $(k = 1, 2)$ are the standard forward, backward finite differences with respect to the $k$-th components, and $\epsilon$ is a small positive number which is used to prevent the numerical blow-up when

$$\sqrt{|D_1^+ u_{i,j}|^2 + |D_2^+ u_{i,j}|^2} = 0,$$

which is a standard treatment in all TV based numerical schemes in the literature.

(iii) Compute the curvature projections onto the wavelet basis by

$$\text{WCURV} = \text{FWT}(\text{curv}), \tag{9}$$

where FWT is the forward wavelet transform.

Then we are ready to give a complete algorithm.

**Algorithm:**

(1) Start with $n = 0$ and initial guess $\beta_{j,k}^{new} = \alpha_{j,k}\chi_{j,k}$, where $\chi_{j,k}$ is the characteristic function of inpainting regions $I$, i.e.

$$\chi_{j,k} = \begin{cases} 1 & (j,k) \in I \\ 0 & (j,k) \notin I \end{cases},$$

Set $\beta_{j,k}^{old} = 0$, and the initial error $E = \|\beta^{new} - \beta^{old}\|_2$.

(2) While $i \leq N$ or $E \leq \delta$, do

- Set $\beta^{old} = \beta^{new}$.
- Calculate $\beta^{TV} = \text{WCURV}$ by Procedure I.
- For all $(j, k)$, update

$$\beta_{j,k}^{new} = \beta_{j,k}^{old} + \frac{\Delta_t}{\Delta_x} \gamma_{j,k},$$

with $\gamma_{j,k}$ defined by

$$\gamma_{j,k} = \beta_{j,k}^{TV} - 2\lambda(\beta_{j,k} - \alpha_{j,k})(1 - \chi_{j,k}),$$

where $\Delta_t, \Delta_x$ are temporal and spatial step sizes respectively.

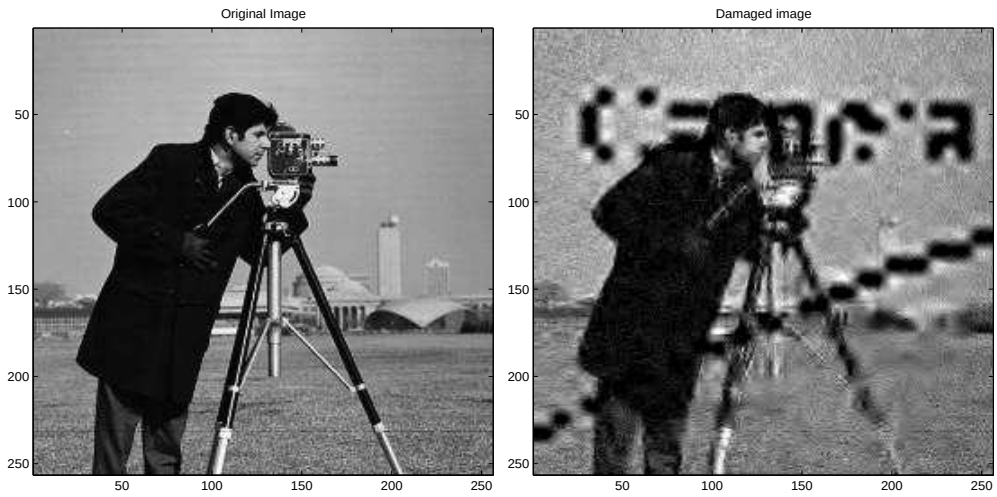


Figure 1: Left: Original Cameraman image. Right: Image reconstructed with damaged wavelet coefficients , including some low frequency ones, which results in large damaged regions in the pixel domain. Notice that there are no well defined inpainting regions in the pixel domain. PSNR $= 15.29(dB)$.

- Compute error $E = \|\beta^{new} - \beta^{old}\|_2$, and set $i = i + 1$.
- End the while loop.

We remark that there are many methods available in the literature to find the minimizers of the proposed models (e.g., properly modifying the lagged-diffusivity fixed point iterative schemes [1, 19]). By no means the time marching scheme in this paper is the most efficient.

To test the model with the multilevel fitting parameters, we apply the above algorithm to a standard Cameraman image shown on the left of Figure 1. The classical Daubechies 7-9 biorthogonal wavelet is employed throughout the computation. In addition to the visual quality comparison, we compute the standard Peak Signal to Noise Ratio (PSNR) to quantify the performance of inpainting:

$$\text{PSNR} = 10\log_{10}(\frac{255^2}{\|u - u_0\|_2^2})(dB),$$

where 255 is the maximum intensity value of gray scale images, $u_0$ the noise free original image, and $\|\cdot\|_2$ the standard $L^2$ norm. As usual, larger PSNR values signifies better performance.

We show the inpainting regions in the wavelet domain by a frequency index set picture plotted in Figure 2. The frequency indexes have been arranged in the standard manner with upper left corner storing the low-low frequencies, and lower right portion the high-high ones. Every black point in the frequency index set picture indicates the corresponding wavelet coefficient being lost. We note that the inpainting regions in the wavelet domain is not random, which differs from the examples presented in [14]. And there are large connected regions, such as the black texts, to be inpainted. The picture on the right (PSNR $= 15.29(dB)$) is obtained by losing (setting to zero) the wavelet coefficients according to the frequency index set picture. It is easy to observe that there are no well defined inpainting regions in the pixel domain. The damaged low-resolution components results in the chunky black "lines" and "spots" in the middle of the image. Moreover, different regions have different severity of damage which are certainly inhomogeneous in the pixel domain.

The inpainted images using our Model are plotted in Figure 3. We show the inpainted image with constant $\lambda = 25$ on the left (PSNR $= 23.77(dB)$) and with multilevel $\lambda$ values for different frequency ranges on the right (PSNR $= 23.83(dB)$). In addition to the clear improvement measured by PSNR, both images improve the visual quality dramatically well. They fill in the inhomogeneous damaged black regions properly while removing the noise. More importantly, they perform surprisingly well in restoring the geometrical features, such as the sharp edges on the tower and the body, and the shapes of head and camera.


Figure 2: The frequency index set picture shows the locations (black) of missing wavelet coefficients. The upper left corner stores the low-low frequencies and the lower right portion the high-high ones.

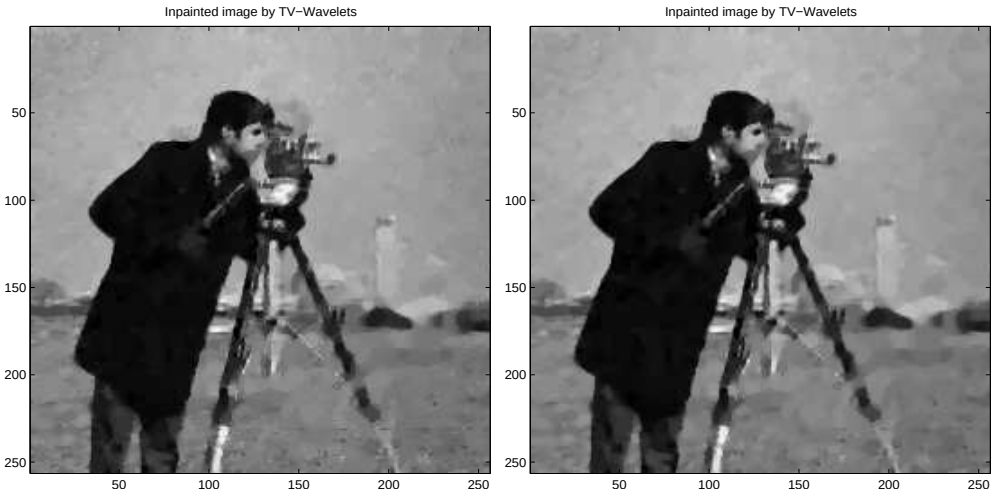


Figure 3: Inpainted images by the TV wavelet inpainting model. Left: constant $\lambda = 25$ resulting PSNR $= 23.77(dB)$. Right: multilevel fitting parameter $\lambda = 50, 35, 25, 17.6$ for different (from low to high) frequency subbands respectively. PSNR $= 23.83(dB)$. Both inpainted images surprisingly restore the large damaged regions while removing the noise. More importantly, they retain and reconstruct the geometrical information such as sharp edges of the body and the tower in the image.

## References


[1] R. Acar and C. R. Vogel. Analysis of total variation penalty methods for ill-posed problems. *Inverse Prob.*, 10:1217–1229, 1994.

[2] C. Ballester, M. Bertalmio, V. Caselles, G. Sapiro and J. Verdera, *Filling-in by Joint Interpolation of Vector Fields and Grey Levels*, IEEE Trans. Image Processing, 10(8), 2001, 1200-1211.

[3] M. Bertalmio, A.L. Bertozzi, and G. Sapiro. *Navier-Stokes, fluid dynamics, and image and video inpainting*, 2001 IEEE Conference on Computer Vision and Pattern Recognition. December. Kauai, Hawaii. Available at http://www.ece.umn.edu/users/marcelo/final-cvpr.pdf.

[4] M. Bertalmio, G. Sapiro, V. Caselles and C. Ballester, *Image Inpainting,* Tech. Report, ECE-University of Minnesota, 1999.

[5] M. Bertalmio, L. Vese, G. Sapiro and S. Osher, *Simultaneous Structure and Texture Image Inpainting*, UCLA CAM Report 02-47, July 2002,

[6] E. J. Candès, and F. Guo. *Edge-preserving Image Reconstruction from Noisy Radon Data*, (Invited *Special Issue of the Journal of Signal Processing on Image and Video Coding Beyond Standards.*), 2001.

[7] E. Candès, J. Romberg and T. Tao, *Robust Uncertainty Principles: Exact Signal Reconstruction from Highly Incomplete Frequency Information*, Preprint: arXiv:math.GM/0409186, Sept. 2004.

[8] E. Candès, and T. Tao, *Near Optimal Signal Recovery From Random Projections and Universal Encoding Strategies*, Preprint, submitted to IEEE Information Theory, Oct. 2004.

[9] V. Caselles, R. Kimmel and G. Sapiro, *On Geodesic Active Contours*, Int. Journal of Computer Vision, 22(1), 1997, 61-79.

[10] A. Chambolle, R. A. DeVore, N.-Y. Lee, and B. J. Lucier. *Nonlinear wavelet image processing: variational problems, compression and noise removal through wavelet shrinkage*. IEEE Trans. Image Processing, 7(3):319–335, 1998.

[11] T. F. Chan, S. H. Kang and J. Shen, *Euler's Elastica and Curvature Based inpainting*, SIAM J. Appl. Math., 63(2) (2002), 564-592.

[12] T. F. Chan and J. Shen, *Mathematical Models for Local Non-Texture Inpainting*, SIAM J. Appl. Math., 62(3) (2002), 1019-1043.

[13] T. F. Chan and J. Shen, *Morphologically Invariant PDE Inpaintings*, UCLA CAM Report 01-15, 2001.

[14] T. F. Chan, J. Shen, and H. M. Zhou, *Total Variation Wavelet Inpainting*, to appear in J. of Math. Imaging and Vision.

[15] T. F. Chan and L. Vese, *Active Contour Without Edges* Submit to IEEE Tran. on Image Proc., 1998.

[16] T. F. Chan and C. K. Wong, *Total Variation Blind Deconvolution*, IEEE Trans. Image Processing, 7 (1998), pp. 370-375.

[17] T. F. Chan and H. M. Zhou, *Optimal Constructions of Wavelet Coefficients Using Total Variation Regularization in Image Compression*, CAM Report, No. 00-27, Dept. of Math., UCLA, July 2000.

[18] L. Demanet, B. Song and T. Chan, *Image Inpainting by Correspondence Maps: a Deterministic Approach*, UCLA CAM Report 03-40, August 2003.

[19] D. Dobson and C.R. Vogel, *Convergence of An Iterative Method for Total Variation Denoising*, SIAM Journal on Numerical Analysis, 34 (1997), pp. 1779-1971.

[20] D. Dugatkin, H. M. Zhou, T. F. Chan and M. Effros, *Lagrangian Optimization of A Group Testing for ENO Wavelets Algorithm*, Proceedings to the 2002 Conference on Information Sciences and Systems, Princeton University, New Jersey, March 20 - 22, 2002.

[21] S. Durand and J. Froment, *Artifact Free Signal Denoising with Wavelets*, in Proceedings of ICASSP'01, volume 6, 2001, pp. 3685-3688.

[22] M. Elad, J-L. Starck, P. Querre and D. Donoho, *Simultaneous Cartoon and Texture Image Inpainting Using Morphological Component Analysis (MCA)*, to appear in the J. on Applied and Computational Harmonic Analysis.

[23] S. Esedoglu and J. Shen. Digital inpainting based on the Mumford-Shah-Euler image model. *European J. Appl. Math.*, 13:353–370, 2002.

[24] H. Igehy and L. Pereira, *Image Replacement Through Texture Synthesis*, Proceedings to IEEE ICIP, 1997.

[25] K.-H. Jung, J.-H. Chang, and C. W. Lee, *Error Concealment Technique Using Data for Block-Based Image Coding*, SPIE, 2308,(1994), 1466-1477.

[26] Sung Ha Kang, Tony F. Chan and Stefano Soatto, *Inpainting from Multiple View*, UCLA CAM Report 02-31, May 2002.

[27] F. Malgouyres, *Mathematical Analysis of a Model Which Combines Total Variation and Wavelet for Image Restoration*, Journal of information processes, 2:1, 2002, pp 1-10.

[28] F. Malgouyres and F. Guichard, *Edge Direction Preserving Image Zooming: a Mathematical and Numerical Analysis*, SIAM, J. Num. Anal., 39:1, 2001, pp 1-37.

[29] L. Moisan, *Extrapolation de Spectre et Variation Totale Ponderee*, actes du GRETSI, 2001.

[30] M. Masnou and J. Morel, *Level-lines Based Disocclusion*, IEEE ICIP, October, 1998, 259-263.

[31] D. Mumford and J. Shah. *Optimal approximations by piecewise smooth functions and associated variational problems.* Comm. Pure Applied. Math., 42:577–685, 1989.

[32] M. Nitzberg, D. Mumford, and T. Shiota. *Filtering, Segmentation, and Depth.* Lecture Notes in Comp. Sci., Vol. 662. Springer-Verlag, Berlin, 1993.

[33] L. Rudin, S. Osher and E. Fatemi, *Nonlinear Total Variation Based Noise Removal Algorithms*, Physica D, Vol 60(1992), pp. 259-268.

[34] J.L. Starck, M. Elad and D. Donoho. *Image Decomposition via the Combination of Sparse Representations and a Variational Approach.* to appear in the IEEE Trans. Image Processing.

[35] David M. Strong, Peter Blomgren, and Tony F. Chan, *Spatially Adaptive Local Feature-Driven Total Variation Minimizing Image Restoration*, Proceedings of SPIE, vol. 3167, 1997, pp. 222-233 .

[36] Y. Wang, and Q. F. Zhu, *Error Control and Concealment for Video Communication: A Review*, Proc. IEEE, vol 86, no. 5, pp. 974-997.

[37] A. Yezzi, A. Tsai and A. Willsky, *A Fully Global Approach to Image Segmentation via Coupled Curve Evolution Equations*, Submitted to Journal of Visual Communication and Image Representation.